

## Microscopic Studies of Polyaniline-poly-*N*-isopropylacrylamide/Alumina Composites Containing Dodecylbenzene Sulfonic Acid

C. Basavaraja, R. Pierson, Ju-Hwang Kim,<sup>†</sup> and Do Sung Huh<sup>\*</sup>

Department of Chemistry and Institute of Functional Materials, Inje University, Kimhae, Kyungnam 621-749, Korea

<sup>\*</sup>E-mail: chemhds@inje.ac.kr

<sup>†</sup>Division of Advanced Technology, Korea Research Institute of Standards and Science, Yuseong, Daejeon 303-340, Korea

Received June 6, 2008

The polyaniline (PANI) composites containing poly(*N*-isopropylacrylamide-co-acrylic acid/alumina) (PNA/Al<sub>2</sub>O<sub>3</sub>) were synthesized by chemical polymerization of aniline in an aqueous solution containing dispersed PNA/Al<sub>2</sub>O<sub>3</sub> in the presence of dodecylbenzene sulfonic acid (DBSA). The topography of obtained composites was investigated with scanning electron microscopy (SEM) and atomic force microscopy (AFM). Thermal stability was reassessed by thermogravimetric (TGA) and differential scanning calorimetry (DSC). A correlation in the surface modification of the composite between Al<sub>2</sub>O<sub>3</sub> and PANI-PNA has been discussed.

**Key Words :** Conducting polymer, Polymer composite. Polyaniline, Polyaniline-poly-*N*-isopropylacrylamide-co-acrylic acid/alumina (PANI-PNA/Al<sub>2</sub>O<sub>3</sub>)

### Introduction

Among the conductive polymers, polyaniline (PANI) occupies a place of special interest. PANI has many advantages: relatively cheap, easy to synthesize, environmental stability, and controllable conductivity, so the PANI is regarded as the most promising conducting polymer material for commercial application.<sup>1</sup> However, PANI exhibits lower thermal stability, processibility, and electric properties in comparison with inorganic conducting materials or coating materials.<sup>1-4</sup> A large amount of PANI-inorganic composites have been synthesized and studied to enhance the overall properties and broadening the practical applications in the past few years.<sup>5-13</sup> The inherent stability of the composite materials is often better than the one component bulk materials mainly because the parent polymer in the composite provides high dispersion and high surface area for the secondary components to integrate, and therefore it creates templates for chemical reactions and interactions for the symbiosis between the two components. The main aspect of concerns is the stabilization of the secondary component in the polymer matrix of composite materials. High percent loading of inorganic materials with the PANI to form composite will decrease an adhesion between the PANI and the inorganic materials during the formation of the composite. Because of this drawback it was not easy to obtain the desired properties of PANI-inorganic composites. There have been a number of attempts to overcome this problem for improving PANI composite by doping with various dopants.<sup>14-18</sup>

It is well known that thermo responsive polymers is easily changing in their physical or chemical properties discontinuously or sharply at or around their lower critical solution temperature (LCST).<sup>19,20</sup> It means that the micro-particles made from such a material will also have some temperature-related properties. The microgels containing poly(*N*-iso-

propylacrylamide) (PNIPAm) were found to exhibit outstanding capabilities as potential carriers and protective containers for biologically active molecules. These microgels possess several advantages over bulk gels in the point of small size and volume, high surface area, faster response to stimuli, and high diffusivity because their size ranges typically from 50 nm to 5  $\mu$ m. Until now, many papers on physico-chemical properties of PNIPAm microgel itself have been published.<sup>21,22</sup> However, the studies on the preparation of thermosensitive composites by precipitation polymerization on sacrificial template core are very few.

The use of dodecylbenzene-sulfonic acid (DBSA), a bulky molecule containing polar head and a long non-polar chain, can affect to the preparation of the composite as a surfactant and dopant. It is also interesting that the use of DBSA in the synthesizing process of the composite influences on the morphology of the composite, particularly by changing the shape and size of PANI particles. The presence of poly(*N*-isopropylacrylamide-co-acrylic acid) (PNA) and DBSA in solution state adsorbs most of aniline monomers onto their complex network. Introduction of acrylic acid (AA) groups in PNA is interesting since carboxy groups promote the adhesion of metal substrates.<sup>23</sup> Polymerization of aniline under these circumstances will help to improve the nature of interaction between PANI-metal particles.<sup>24</sup> Alumina is the most widely used ceramic oxide, in pure form or as raw material to be mixed with other oxides and is available raw material at relatively low price.<sup>25</sup> It has high compression strength, high hardness, resistant to abrasion, resistant to chemical attack by a wide range of chemicals even at elevated temperatures. And also it has high thermal conductivity, resistant to thermal shock, high degree of refractoriness, high dielectric strength, high electrical resistivity even at elevated temperatures, transparent to microwave radio frequencies and low neutron cross section capture area.

In this communication, we report the studies on the PANI-

PNA/Al<sub>2</sub>O<sub>3</sub> composites that are synthesized with different wt.% of Al<sub>2</sub>O<sub>3</sub> in the presence of DBSA. We have used the PNA microgel in the presence of DBSA to obtain a better processability and thermal stability of Al<sub>2</sub>O<sub>3</sub>/PANI composites. The morphological change of chemical interactions being induced by the incorporation of PANI and PNA/Al<sub>2</sub>O<sub>3</sub> were studied by SEM, AFM. Thermal stability was reasserted by TGA and DSC.

### Experimental

**Materials.** AR grade NIPAAm, acrylic acid (AA), potassium persulfate (KPS), aniline, APS, and *N,N*-methylenebisacrylamide (MBA) were purchased from Sigma-Aldrich, while alumina (Al<sub>2</sub>O<sub>3</sub>,  $\alpha$ -form of size 70-80  $\mu$ m) was from Fischer chemicals. DBSA and *N*-methyl-2-pyrrolidinone (NMP) were obtained from Junsei Chemical Co. All solutions were prepared in aqueous media using deionized water.

**Synthesis of PANI-PNA/Al<sub>2</sub>O<sub>3</sub> composite hydrogel films.** Figure 1 shows a schematic model how PANI and Al<sub>2</sub>O<sub>3</sub> can be incorporated into PNA microgels with the help of DBSA surfactant through the free emulsion polymerization method.<sup>21,22</sup> Synthesis of PNA was carried out using the equivalent grade of NIPAAm (0.05 M), AA (0.003 M), MBA (0.002 M), and KPS (0.001 M) in 300 mL deionized water in a three-necked flask at 70 °C under nitrogen atmosphere with vigorous stirring. In case of metal composites, Al<sub>2</sub>O<sub>3</sub> powder was taken in a different (5, 10, 20, and 30) wt.% with respect to aniline concentration and was added to the above mixture. The obtained solution was cooled, and aniline (0.005 M) and DBSA (0.0025 M) were added slowly with constant stirring followed by a drop of APS solution at 0-5 °C. The reaction was carried out for 7-8 h. The growing radical propagates further on the Al<sub>2</sub>O<sub>3</sub> surface and cross-links into a microgel by the copolymerization of PNA monomer and MBA. The -COOH group of AA acts as a

codopant in PNA/Al<sub>2</sub>O<sub>3</sub> microgels and helps to adsorb aniline monomers onto the PNA/Al<sub>2</sub>O<sub>3</sub> microgels. The addition of oxidant (ammonium persulfate, APS) initiates the oxidative polymerization of PANI in the system, and this forms individual PANI particles, which are not deposited into the microgel network rather will be included in the DBSA micelles. This shows how PANI is incorporating into the microgel structure and forming composites.

After then, the resulting precipitate was filtered and washed thoroughly with deionized water and acetone. And it was dried under vacuum for 24 h to achieve a constant weight. The powder was treated with a solution of sodium ethoxide (C<sub>2</sub>H<sub>5</sub>ONa) and ethanol, and was magnetically stirred at room temperature for 12 h. Finally, the precipitate was filtered and washed repeatedly with ethanol and stored in a desiccator for 4 h at room temperature. Later 1-2 g of finely ground powder was taken and added to 30 mL of NMP solution magnetically stirred for 24 h at room temperature. The concentrated solution was then placed into a Petri dish, and the NMP solvent was allowed to evaporate at 45 °C for 48 h. The films with thickness of *ca.* 30  $\mu$ m were placed in distilled water, followed by rinsing with ethanol and drying at room temperature for another 24 h. To obtain solvent-free films, the residual NMP was removed by three cycles of doping using 1 M HCl solution for 18 h and de-doped by 0.1 M NH<sub>4</sub>OH solution for another 18 h at room temperature. The resulting NMP-free composite films were cleaned in deionized water and were dried at room temperature for 24 h.<sup>26</sup>

**Characterization.** The surface morphology of these composite films was investigated by using Philips XL-30 ESEM scanning electron microscopy. Atomic force microscopy (AFM) was performed on a commercial Digital TESP7 VEECO Instruments using optical beam deflection to monitor the displacement of a microfabricated silicon cantilever having a spring constant of 42 N/m. The etched silicon probes mounted on cantilevers in the tapping mode to avoid surface damage. Typical interaction forces were 10<sup>-9</sup> N. This method minimized surface contact and lateral forces by oscillating the cantilever at 320 kHz ( $\approx$  1 nm root mean square), resulting in a significant improvement of lateral resolution on soft surfaces. The 1  $\mu$ m scans were acquired by scanning the sample in air at 25 °C at a scan rate of 1 Hz and all the scans were 1  $\mu$ m and 500 nm in size. Thermal properties were obtained by TGA (Perkin Elmer model TGA 7) and DSC by (Perkin Elmer model DSC 7) in the range 30-700 °C at 10 °C/min in nitrogen atmosphere.

### Results and Discussion

**Surface morphology studies.** The morphology for a composite is very important to understand the filler (dispersed phase) distribution in the matrix (continuous phase) because it is the most important aspect which governs different physical and mechanical properties. The SEM analysis of PANI-PNA allows for the observation of a peculiar experimental feature. Figure 2(a-c) shows the SEM of PANI-PNA.

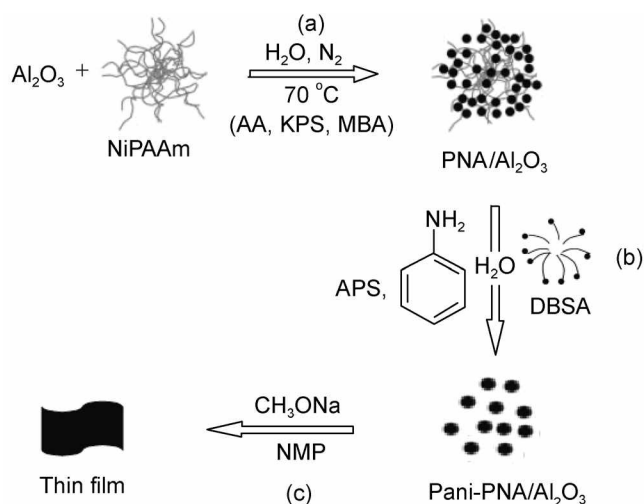


**Figure 1.** Schematic model for the polymerization of PANI in the presence of PNA/Al<sub>2</sub>O<sub>3</sub> microgels. (a) Incorporation of Al<sub>2</sub>O<sub>3</sub> into the PNA matrix (b) Polymerization of aniline in the presence of DBSA and PNA/Al<sub>2</sub>O<sub>3</sub>. (c) Formation of PANI-PNA/Al<sub>2</sub>O<sub>3</sub> thin films.

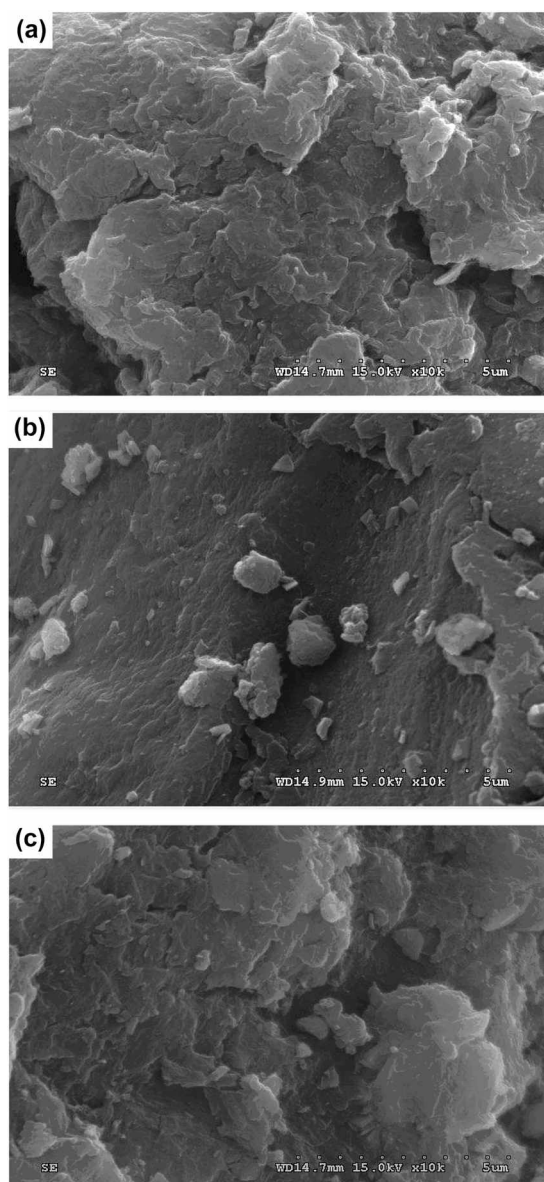


**Figure 2.** Scanning electron micrographs for (a) PANI-PNA, (b) PANI-PNA/Al<sub>2</sub>O<sub>3</sub> (10%), and (c) PANI-PNA/Al<sub>2</sub>O<sub>3</sub> (30%) films.

PANI-PNA/Al<sub>2</sub>O<sub>3</sub> (10%), and PANI-PNA/Al<sub>2</sub>O<sub>3</sub> (30%) films, respectively. The dispersed morphology could be witnessed by the figures. The surface of PANI-PNA is smooth and homogeneous as the composite films form uniform distributions of PANI particles over the surface of PNA. The presence of encapsulated Al<sub>2</sub>O<sub>3</sub> particles in the PANI-PNA/Al<sub>2</sub>O<sub>3</sub> (10%) and PANI-PNA/Al<sub>2</sub>O<sub>3</sub> (30%) creates/makes a fine distribution of cenosphere-like structures in the composite films. In case of PANI-PNA/Al<sub>2</sub>O<sub>3</sub> (10%) it looks as if the beads are floating over the water surface. With increasing amount of Al<sub>2</sub>O<sub>3</sub> (Figure 2(c)) larger size aggregates are visible, suggesting intermixing of Al<sub>2</sub>O<sub>3</sub> particles with the PANI-PNA.<sup>27,28</sup> From the SEM images it is clear that the morphologies of PANI-PNA polymer films became denser and more compact with the increase in the content of Al<sub>2</sub>O<sub>3</sub>. It suggests that the morphological differences could be due

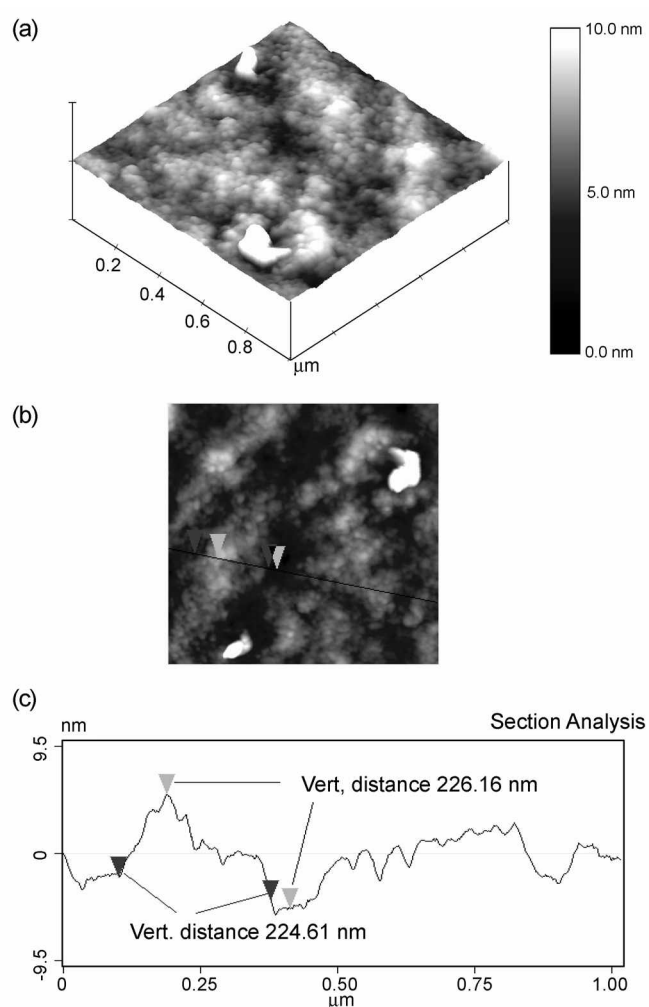


**Figure 3.** AFM images of (a) 3-dimensional and (b) 2-dimensional, and (c) section plots of 1  $\mu$ m of PANI-PNA films.

to an effect of the Al<sub>2</sub>O<sub>3</sub> concentration affecting to the bonding occurs in aqueous dispersion that interfere the interaction between the chains.

Figures 3, 4, and 5 show AFM images of three dimensional, surfaces and section analysis of PANI-PNA, PANI-PNA/Al<sub>2</sub>O<sub>3</sub> interfaces resulting from different initial concentration of Al<sub>2</sub>O<sub>3</sub> namely 10% and 30%. These scans were acquired at 1  $\mu$ m by scanning the sample in air at 25  $^{\circ}$ C at a scan rate of 1 Hz. Figure 3(a) shows the three dimensional image of PANI-PNA, it appears from the figure that the surface of PANI-PNA is fairly smooth and amorphous surface in the form of small and equally distributed, in which narrow features are repeated units along the whole sample and the height of these features is about 10 nm. This can be further evidenced by the surface analysis which is indicated in Figure 3(b). Further the sectional analysis of the PANI-PNA in Figure 3(c) shows the diameter of these narrow features were 225 nm. The three dimensional image of PANI-PNA/Al<sub>2</sub>O<sub>3</sub> (10%) in Figure 4(a) shows the disappearance of narrow features appeared in PANI-PNA due to the incorporation of Al<sub>2</sub>O<sub>3</sub>. Figure 4(b) shows the surface analysis clearly showing the formation of a rough surface.

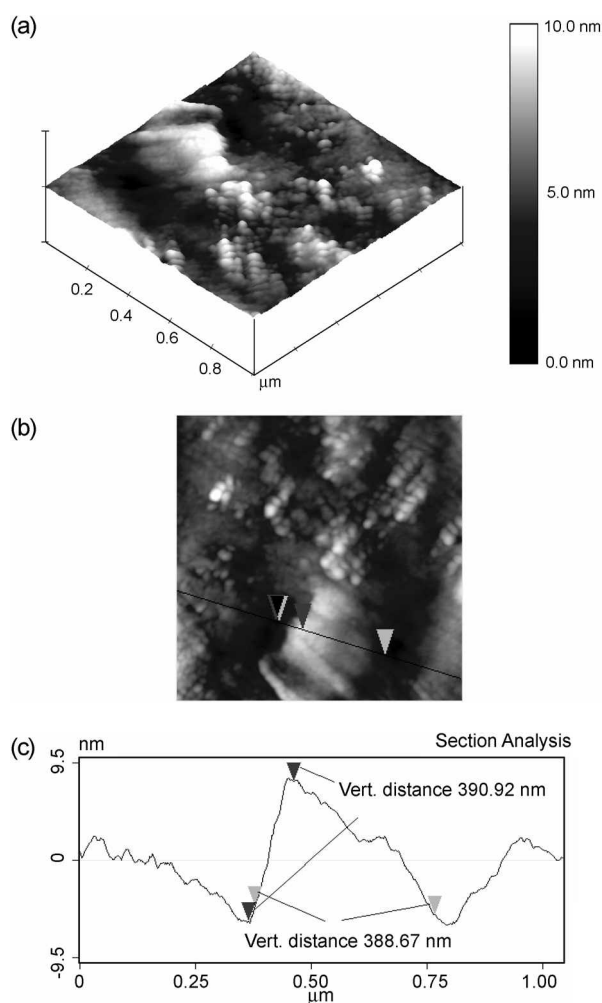


**Figure 4.** AFM images of (a) 3-dimensional and (b) 2-dimensional, and (c) section plots of 1  $\mu\text{m}$  of PANI-PNA/ $\text{Al}_2\text{O}_3$  (10%) films.

The surface becomes fairly rough with no change in the height. However the diameter of has changed to 390 nm, which can be seen as shown in Figure 4(c). Further increase in the concentration of  $\text{Al}_2\text{O}_3$  has changed the surface much more as once can see from the three dimensional image as shown in Figure 5(a) and the surface analysis in 5(b) with a change in the height 30 nm. The sectional analysis in Figure 5(c) also shows the change in the diameter of the polymer which changed to 480 nm.

A comparison of the section plots between Figure 3(c), Figure 4(c), and Figure 5(c) well shows the flattening or broadening of surface features by increasing the content of  $\text{Al}_2\text{O}_3$ . The nano-cavities formed in PANI-PNA disappear at higher concentration of alumina due to the increase in surface density of PANI-PAA/ $\text{Al}_2\text{O}_3$  films. Figure 6 shows the RMS roughness values for various interfaces increasing with the increase of  $\text{Al}_2\text{O}_3$  density. The value of RMS roughness for the pure PANI-PAA is 2.7, increases by the increase of  $\text{Al}_2\text{O}_3$  from 10% to 30% as 3.6 and 8.9, respectively. Thus the surface uniformity in terms of distribution of features and feature size is significantly improved by the incorporation of  $\text{Al}_2\text{O}_3$  in PANI-PAA matrix. The function of AA is

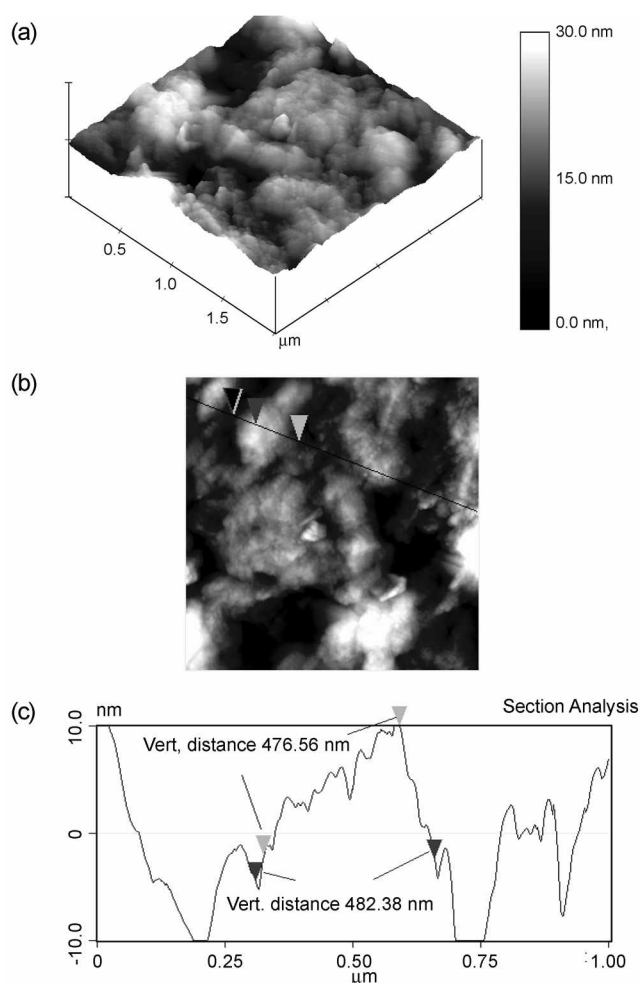


**Figure 5.** AFM images of (a) 3-dimensional and (b) 2-dimensional, and (c) section plots of 1  $\mu\text{m}$  of PANI-PNA/ $\text{Al}_2\text{O}_3$  (30%) films.

increasing the introduction of the PANI-PAA matrix onto  $\text{Al}_2\text{O}_3$  surface because the bonds of AA on alumina surface could react internally with the growing PNIPAm radicals during the polymerization. The surface modification of PANI-PNA/ $\text{Al}_2\text{O}_3$  by AA seems essential to avoid the preparation of pure polymer particles containing no  $\text{Al}_2\text{O}_3$  core. This is because PNA is water-insoluble at the polymerization temperature of 70  $^\circ\text{C}$ , so the growing polymer radical prefers precipitating onto the  $\text{Al}_2\text{O}_3$  surface with the help of AA, when it reaches the critical length in water. The growing radical propagates further on the  $\text{Al}_2\text{O}_3$  surface and cross-links into a microgel by the copolymerization of PNA monomer and MBA.

**Thermal characterizations.** The TGA curves and DSC thermograms of PANI-PNA, PANI-PNA/ $\text{Al}_2\text{O}_3$  (10%), and PANI-PNA/ $\text{Al}_2\text{O}_3$  (30%) are shown in Figures 7 and 8, respectively. The TGA curves of these samples exhibit three steps of mass losses as shown in Figure 7. The initial loss below 100  $^\circ\text{C}$  is assigned to the gradual evaporation of moisture and PNA. The second loss around 250-500  $^\circ\text{C}$  is due to the thermo-chemical decomposition of the chemically active organic materials at this range: DBSA mainly at 150-300 and 250-500  $^\circ\text{C}$ . Above this temperature, degradation

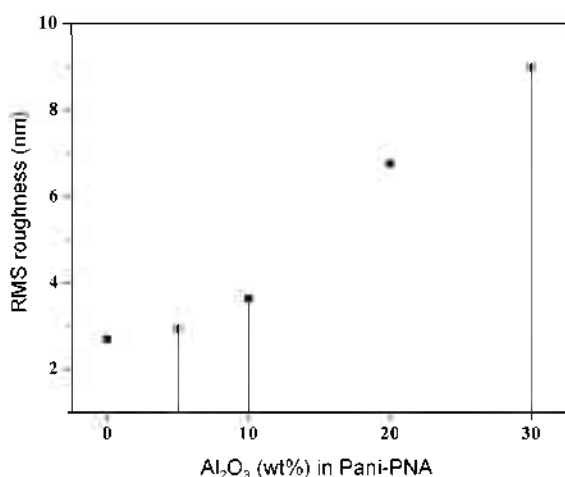


Figure 6. RMS roughness values of PANI-PNA surface with increasing Al<sub>2</sub>O<sub>3</sub> density.

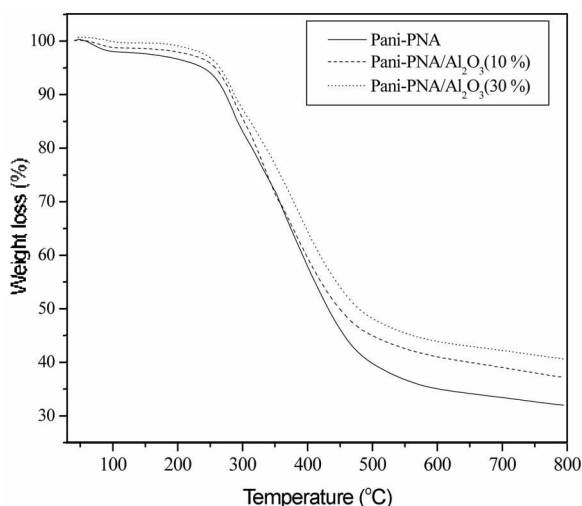


Figure 7. TGA curve of PANI-PNA, PANI-PNA/Al<sub>2</sub>O<sub>3</sub> (10%), and PANI-PNA/Al<sub>2</sub>O<sub>3</sub> (30%) films.

proceeds rapidly. The third stage starts in the range of 500–600 °C, which implies a complete decomposition of organic polymers leaving only the oxide particles whose degradation occurs at a higher temperature. The mass loss for PANI-PNA and PANI-PNA/Al<sub>2</sub>O<sub>3</sub> is very steady under 500 °C, which slightly increases with the increase in the content of Al<sub>2</sub>O<sub>3</sub>. The incorporation of Al<sub>2</sub>O<sub>3</sub> in the polymer matrix shows increased thermal stability. PANI-PNA show a residual weights of 35% at 600 °C, which increases after the introduction of Al<sub>2</sub>O<sub>3</sub> into PANI-PNA. The PANI-PNA/Al<sub>2</sub>O<sub>3</sub> (10%) matrix shows residual weights of 41%, which subsequently increases to 45% for the PANI-PNA/Al<sub>2</sub>O<sub>3</sub> (30%) composite. So, with the increase in Al<sub>2</sub>O<sub>3</sub> concentration as the relative quantity of Al<sub>2</sub>O<sub>3</sub> is increased, the initial weight loss is also increased, as well as left over residue at the end of experiment at 700 °C.

There are three endothermic peaks in the curves of Figures 8(a) and 8(b) of DSC for PANI-PNA, PANI-PNA/Al<sub>2</sub>O<sub>3</sub> (10%). The first one is at 50–160 °C because of the removal

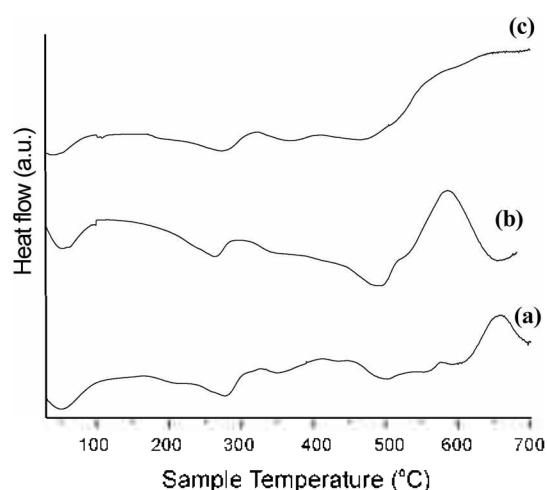


Figure 8. Differential scanning calorimetry thermograms for (a) PANI-PNA, (b) PANI-PNA/Al<sub>2</sub>O<sub>3</sub> (10%), (c) PANI-PNA/Al<sub>2</sub>O<sub>3</sub> (20%), and PANI-PNA/Al<sub>2</sub>O<sub>3</sub> (30%) films.

of moisture/PNA. The second at 280–450 °C results from the removal of DBSA. The third at 500–600 °C is due to the complete removal of chemically active organic molecules. Figure 8(c) for PANI-PNA/Al<sub>2</sub>O<sub>3</sub> (30%) differs significantly from Figures 8(a) and 8(b), as these endothermic peaks is minimized due to the higher content of oxide particles confirming the structural changes after the incorporation of Al<sub>2</sub>O<sub>3</sub>. Since the degradation process of Al<sub>2</sub>O<sub>3</sub> is much higher than that of the polymer matrix, it does not appear in the degradation curve. The higher thermal degradation of composites after the incorporation of Al<sub>2</sub>O<sub>3</sub> indicates that it has a positive influence on the thermal stability of the composites and inhibits their fast degradation.

Composite materials have an improved thermal stability and solution processability compared to each individual component. In spite of shifting of temperature range for all steps to higher values, the composite containing polyaniline in the present case has a beneficial effect on thermal behavior of composites. There is a considerable change in surface modification and thermal decomposition temperature of base polymer due to addition of Al<sub>2</sub>O<sub>3</sub>. The change in thermal properties with the increase in Al<sub>2</sub>O<sub>3</sub> concentration is due to the restricted mobility of the polymer chain imposed by the filler. Al<sub>2</sub>O<sub>3</sub> is acting as reinforcing filler for the matrix and does not deteriorate the mechanical properties like other nonreinforcing fillers. This is mainly because the growing radical propagates further on the Al<sub>2</sub>O<sub>3</sub> surface and cross-links into a microgel by the copolymerization of PNA monomer and MBA. The surface modification of PANI-PNA/Al<sub>2</sub>O<sub>3</sub> by AA avoids the preparation of pure polymer particles containing no Al<sub>2</sub>O<sub>3</sub> core.

## Conclusion

PANI particles are incorporated in a soft and hydrogel matrix made from the chemically crosslinked PNA along with Al<sub>2</sub>O<sub>3</sub> in the presence of DBSA. In this way a new

composite material is synthesized by using a hydrogel as matrix and PANI particles as filler along with inert oxide particles. The microscopic analysis reveals that  $Al_2O_3$  particles dispersed in the polymer matrix, with a tendency to organize into two-dimensional structures. We believe that the new composites synthesized in this way will overcome the problem of phase separation by improving the adhesion between PANI and its inorganic counter part in the composite, which will induce process and reliability concerns of embedded applications of these composites. PNA is bio-compatible which improves the processability of PANI without any significant loss in electrical conductivity. Poly-aniline is an electro active polymer, which exists in different reversible forms having different electrical and optical properties. This feature makes it a very promising material for opto-electronic applications.

**Acknowledgments.** This work was supported by the Korea Research Foundation Grant funded by the Korean Government (MOEHRD) (KRF-00042007070-00).

### References

- Nascimento, G. M.; Constantino, V. R. L.; Temperini, M. L. A. *Macromolecules* **2002**, *35*(20), 7535.
- Feller, J. F.; Bruzaud, S.; Grohens, Y. *Mater. Lett.* **2004**, *58*(5), 739.
- Ray, S. S.; Okamoto, M. *Prog. Polym. Sci.* **2003**, *28*(11), 1539.
- Negi, Y. S.; Adhyapak, P. V. *J. Macromol. Sci.-Polym. Rev.* **2002**, *C42*(1), 35.
- Wu, C. G.; Liu, Y. C.; Hsu, S. S. *Synth. Met.* **1999**, *102*(1-3), 1268.
- Gurunathan, K.; Trivedi, D. C. *Mater. Lett.* **2000**, *45*(5), 262.
- Gurunathan, K.; Amalnerkar, D. P.; Trivedi, D. C. *Mater. Lett.* **2003**, *57*(9-10), 1642.
- Li, X.; Wang, G.; Li, X.; Lu, D. *Appl. Surf. Sci.* **2004**, *229*(1-4), 395.
- Khiew, P. S.; Huang, N. M.; Radiman, S.; Ahmad, M. S. *Mater. Lett.* **2004**, *58*(3-4), 516.
- Basavaraja, C.; Choi, Y. M.; Park, H. T.; Huh, D. S.; Lee, J. W.; Revanasiddappa, M.; Raghavendra, S. C.; Khasim, S.; Vishnuvardhan, T. K. *Bull. Korean Chem. Soc.* **2007**, *28*(7), 1104.
- Xiao, P.; Xiao, M.; Liu, P.; Gong, K. *Carbon* **2000**, *38*(4), 626.
- Anaissi, F. J.; Demets, G. J. F.; Timm, R. A.; Toma, H. E. *Mater. Sci. and Eng.* **2003**, *A347*(1-2), 374.
- Ilic, M.; Koglin, E.; Pohlmeier, A.; Narres, H. D.; Schwuger, M. J. *Langmuir* **2000**, *16*(23), 8946.
- Orata, D.; David, S. K. *Reactive & Functional Polymers* **2000**, *43*(1-2), 133.
- Orata, D.; Segor, F. *Reactive & Functional Polymers* **2000**, *45*(3), 305.
- Kim, B. H.; Jung, J. H.; Kim, J. W.; Choi, H. J.; Joo, J. *Synt. Met.* **2001**, *121*(1-3), 1311.
- Kim, B. H.; Jung, J. H.; Kim, J. W.; Choi, H. J.; Joo, J. *Synt. Met.* **2001**, *117*(1-3), 115.
- Yang, S. M.; Chen, K. H. *Synt. Met.* **2003**, *135*, 51.
- Basavaraja, C.; Park, D. Y.; Choe, Y. M.; Park, H. T.; Zhao, Y. S.; Yamaguchi, T.; Huh, D. S. *Bull. Korean Chem. Soc.* **2007**, *28*(5), 805.
- Yoshida, R.; Kokufuta, E.; Yamaguchi, T. *Chaos* **1999**, *9*(2), 260.
- Basavaraja, C.; Pierson, R.; Vishnuvardhan, T. K.; Huh, D. S. *Env. Poly. J.* **2008**, *44*, 1556.
- Lung, L. C.; Yen, C. W.; Fen, L. C. *J. Poly. Sci.: A Poly. Chem.* **2006**, *44*, 356.
- Yang, T. C. K.; Tsai, S. H. Y.; Wang, S. F.; Juan, C. C. *Composite Sci. Technol.* **2002**, *62*, 655.
- Basavaraja, C.; Pierson, R.; Huh, D. S. *J. App. Poly. Sci.* **2008**, *108*, 1070.
- Chongfu Zhou, Tao Liu, Tong Wang, Kumar, S. *Polymer* **2006**, *47*, 5831.
- Liu, Y.; O'Keefe, M. J.; Beyaz, A.; Thomas, P. S. *Surface and Interface Analysis* **2005**, *37*, 782.
- Vecino, M.; Gonzalez, I.; Munoz, M. E.; Santamaria, A.; Ochoteco, E.; Pomposo, J. A. *Polym. Adv. Technol.* **2004**, *15*, 560.
- Raghavendra, S. C.; Khasim, S.; Revanasiddappa, M.; Ambikapradas, M. V. N.; Kulkarni, A. B. *Bull. Mat. Sci.* **2003**, *26*(7), 733.